

Implementation of a High Resolution Stepped Frequency Radar on a USRP

Venceslav Kafedziski, Senior Member, IEEE, and Sinisha Pecov

Abstract—We implement a software defined stepped frequency radar using a USRP. Stepped frequency radar suffers from large data collection time due to large number of pulses with different frequencies sent. Our approach uses a baseband stepped frequency signal, which is upconverted to RF, and, then, frequency hopping the RF frequency. In this way, a low cost hardware with moderate instantaneous RF bandwidth can be used. The total time for hopping all the frequencies, i.e. the data collection time, is also reduced. Resolution can be improved many-fold, depending on the USRP total frequency range.

Keywords—High Resolution Radar, Stepped frequency radar, Software Defined Radar, USRP, GNU Radio.

I. INTRODUCTION

Radar is an object-detection system that uses radio waves to determine the position and velocity of objects. It can be used to detect weather formations, motor vehicles, ships, aircraft, spacecraft, and even terrain. A radar system consists of a transmitter producing electromagnetic waves in the UHF or microwaves domain, a transmitting antenna, a receiving antenna, and a receiver and processor to determine properties of the object. Radio waves radiated from the transmitter reflect off the object and return to the receiver, giving information about the object's location and velocity. Two main radar categories for range detection are the pulsed radar, where very short pulses are transmitted, and the Continuous Wave (CW) radar, where a continuous wave of a changing frequency (usually a Linear Frequency Modulated (LFM) CW signal, or "chirp" signal) is transmitted [1]. In both cases, radar resolution depends on the bandwidth used. In the first case, to increase resolution, the pulse duration is reduced, which requires increased bandwidth. In the second case, the difference between the maximum and minimum frequency of the LFM-CW signal determines the bandwidth, and, to increase resolution, the bandwidth has to be increased. There is another approach, called a stepped frequency (SF) radar, where pulses of different frequencies (usually frequencies of the consecutive pulses differ by an equal amount, the frequency step) are sent, and the returns are measured [2]–[4]. With the step going to zero, this approach turns into the LFM-CW approach. The main advantage of the SF radar is the reduced instantaneous RF bandwidth, since the bandwidth depends on the pulse duration only. The resolution depends reciprocally on the total bandwidth, which in turn depends on the total number of pulses with different frequencies used and the frequency step. The main drawback of the SF radar

is the increased time to send all the pulses, which results in increased measurement time. On the other hand, processing can be done after collecting all the measurements, i.e. it does not have to be in real time. Since the RF circuit cannot change the frequencies instantaneously (i.e. it requires some setting time), this approach requires a long data collection time. One solution to this problem could be to generate a baseband SF signal, and then upconvert to RF frequency. But, in this case, in order to increase resolution, the RF bandwidth has to be very large (at least twice the bandwidth of the baseband SF signal). Hardware with such a large RF bandwidth (of the order of one to few GHz) can be very expensive.

In order to implement our radar system (both the transmitter and the receiver) we use the National Instruments (NI) Universal Software Radio Peripheral (USRP), which is a Software Defined Radio (SDR) product. Thus, we implement a Software Defined Radar. There is an extensive literature on the Software Defined Radar using the USRP, such as [5], [6], but usually LFM-CW radars are implemented. Some publications describe the USRP implementation of the SF radar [7], but the focus there is on the Matlab simulation.

The USRP uses a sampling rate of up to 200 MSamples/s and RF daughterboards with an RF bandwidth of up to 160 MHz (baseband of maximum 80 MHz), which does not give the required resolution for some applications, like, for instance, the Ground Penetrating Radar (GPR). In order to increase this bandwidth, we propose to use a SF radar. We combine two approaches, the first using a frequency hopping signal in the baseband, and then upconverting the signal to the RF, and, the second, using a frequency hopping of the RF frequency. In this way, by increasing the radar bandwidth, we increase the resolution of the radar implemented with the first approach. On one hand, our approach dispenses with the need of using an expensive hardware with a very wide RF bandwidth that would be required by a purely baseband frequency hopping approach, and, on the other hand, our approach reduces the necessary time for frequency hopping the entire bandwidth, that would be required by a purely RF frequency hopping approach. Thus, instead of hopping each frequency, we use a frequency hopped baseband signal (a burst), and, then, hop the frequency of the RF carrier in different frequency bands (subbands). In this way, we can arbitrarily increase the radar bandwidth (limited only by the total frequency range of the USRP), and, thus, arbitrarily increase the radar resolution. Our results show that by using only four RF frequencies (i.e. four subbands), the resolution improves significantly.

In our approach we achieved a maximum sampling frequency of 100 MSamples/s, which translated to the maximum baseband frequency of 45 MHz. In order to ensure that each

V. Kafedziski and S. Pecov are with the Faculty of Electrical Engineering and Information Technologies, University Ss Cyril and Methodius, Skopje, Republic of Macedonia (e-mail: kafedzi@feit.ukim.edu.mk, nine_pec@yahoo.com).

RF frequency is properly set, we assumed a time period of around 20 ms between two consecutive bursts.

The paper is organized as follows. In Section II we describe our approach of combining the baseband frequency hopping with RF frequency hopping. We also describe how we solve the problem with the phase jumps that appear at the borders of the adjacent subbands. In Section III we describe the hardware and the software used. In Section IV we describe the measurements setting and the results obtained. Section V concludes the paper.

II. METHOD DESCRIPTION

Assume that the SF radar frequency step is Δf . The radar unambiguous range is given by $R_u = c/(2\Delta f)$, where c is the speed of light. If the number of all the hopped frequencies in the stepped frequency radar is K , the range resolution is given by $R = c/(2K\Delta f)$. We assume a baseband of N hopped frequencies in the burst, and M subbands at M different RF frequencies. Thus, the total number of different frequencies is $K = MN$. The receive chain of the USRP outputs the samples of the demodulated I and Q components from each RF frequency. Since the baseband signal is also obtained by frequency hopping, we still need to demodulate the obtained I and Q components to DC real and imaginary parts. We do this by multiplying the I and Q components with $\cos(2\pi f_i t)$, $0 \leq t \leq \tau$, where $f_i = i\Delta f$, $i = 1, \dots, N$ is the i -th frequency in the burst, and τ is the pulse duration. In the discrete time domain, we have $\cos(2\pi f_i n T_s) = \cos(2\pi (f_i/f_s)n)$, $n = 0, \dots, S-1$, where T_s is the sampling period and f_s is the sampling frequency, and S is the number of samples in the pulse ($\tau = ST_s$). But, since the transmitted pulses of different frequencies in the burst have random phases, and of interest is the phase delay introduced by the propagation of the reflected signal, we demodulate each received pulse in the burst by multiplying it (mixing) with the corresponding transmit pulse in the burst. Thus, we obtain S real numbers for the I component and S real numbers for the Q component, i.e. S complex numbers for each pulse in the burst.

We have tried two approaches, using a lowpass filter (Butterworth, Elliptic) to filter the S complex numbers and summing up the complex numbers at its output, or just summing up the S complex numbers of the downconverter (mixer) output. The second approach implements a matched filter for a rectangular pulse (in fact, a correlation receiver). For each resulting complex sample at each frequency we evaluate its angle and its module. The angle corresponds to the phase delay between the transmitted and the received signal at the corresponding frequency. The module corresponds to the amplitude change at each frequency (since the transmitted pulses are with equal amplitudes). By collecting the complex samples of the matched filter output for all the frequencies in the burst, we obtain the channel transfer function, corresponding to a single subband.

We stack together the complex samples of all M subbands to obtain a vector of $K = MN$ complex samples, and, thus, increase the bandwidth by the factor of M . By taking the inverse DFT of this complex vector, we obtain the range

profile. The size of the IDFT could be $L \geq K$, where the remaining complex samples from $K+1$ to L of the input vector to the IDFT block are zero padded.

Since the RF signal is Double-sideband suppressed-carrier (DSB-SC) signal, we need to adjust the frequencies of the subbands in such a way that the frequency step between the last pulse from the $(j-1)$ th subband and the first pulse from the j th subband is equal to Δf . Thus, $F_j = F_1 + (j-1)N\Delta f$, $j = 1, \dots, M$, where F_1 is the starting RF carrier frequency and F_j is the carrier frequency of the j -th subband, $j = 1, \dots, M$. Within each subband j , $j = 1, \dots, M$, the frequencies are given by $f_{j,i} = F_1 + (j-1)N\Delta f + i\Delta f$, $i = 1, \dots, N$. We use the notation $\Delta F = N\Delta f$.

We checked the validity of our approach by controlling the angles (phases) of the complex samples at the output of the matched filters for all bursts and all subbands. This phase characteristic has to be linear. However, we noticed phase jumps at the borders between the adjacent subbands. This is due to hardware phase changes when setting the different carrier frequencies. In order to remove these phase jumps, we estimated the coefficients of the linear regression of the phase characteristic for each subband, i.e. the slope and the y -intercept. Then we subtracted the y -intercept for each subband from the evaluated values of the phases at different frequencies of that subband. After that, we reevaluated the complex samples for all the frequencies in the burst and all the subbands, and evaluated the inverse DFT to obtain the range profile.

In the stepped frequency radar there are several conditions that have to be met. There is a relationship between the pulse width and the frequency step. In order to avoid aliasing, $\Delta f \leq 1/\tau$, and usually $\Delta f \leq 1/(2\tau)$ is adopted. Also, the pulse repetition interval is usually set to be several times larger than the pulse width, $T = P\tau$, where P is the number of range bins. For each of those bins the inverse DFT of the vector of complex samples of the matched filter outputs of all frequencies is evaluated.

III. HARDWARE AND SOFTWARE DESCRIPTION

The SDR (Software Defined Radio) offers flexibility in the design and implementation of various radio systems. One of the popular tools for implementing SDR is the free and open source software radio development environment called GNU Radio, designed to operate on PC compatible hardware running (primarily) Linux. The hardware counterpart used was NI USRP (Universal Software Radio Peripheral). In this work we used Ettus' X310 USRP with Xilinx Kintex-7 FPGA and CBX-120 RF daughterboard with frequency range 1.2-6 GHz and 120 MHz bandwidth. The USRP was connected to a desktop PC via dual 10 Gigabit Ethernet card and PCI Express interface which could enable sampling rates of up to 200 MS/s (Full Duplex). We used GNU Radio version 3.7.11.1 with GRC (GNU Radio Companion) and UHD (USRP Hardware Driver) API version 3.11.0. As transmit and receive antennas we used a pair of Rohde & Schwarz HL040 Log-Periodic broadband antennas that provide broadband transmission and reception in the frequency range from 400 MHz to 3.6 GHz.

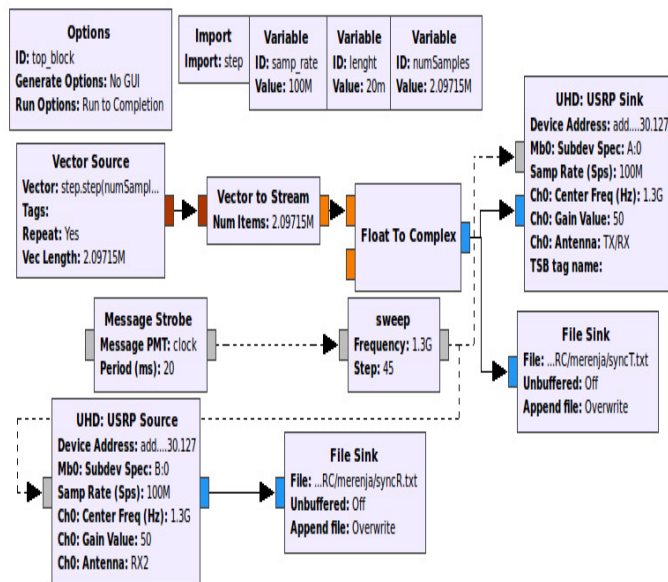


Fig. 1. GRC model - block diagram

We created a GRC model, shown in Fig. 1. In this model we created two Out-Of-Tree (OOT) blocks. The first OOT block generates the desired baseband stepped frequency signal. This block defines the number of frequencies N , the desired frequency step Δf , the pulse duration τ and the pulse repetition interval T . All the parameters can be easily modified. This block is imported in GRC and called in the "Vector Source" block. The "Vector Source" block is connected with the "Vector to Stream" block, which is then connected to "Float to Complex" block so that the desired stream is created. This stream is then sent to the "UHD USRP Sink" block which is the transmitter block. Additionally, the transmitted signal is saved using the "File Sink" block. The receiver "UHD USRP Source" block is connected with the "File Sink" block which stores the received signal. The second OOT block ("Sweep" function) is a control block that sets the desired carrier frequency for both the transmitter and receiver using PMTs (Polymorphic Types) through the flow graph. In this block the initial frequency and the frequency step are defined and controlled by the "Message Strobe" block. The "Message Strobe" defines the time instant when certain carrier frequency is set for both the transmitter and receiver. After that, a time period is added to enable that a new carrier frequency is set for both the transmitter and receiver. After an elaborate testing of this model we concluded that the carrier frequency of transmitter and receiver could be changed every 20 ms without introducing errors. Further investigations are needed to determine the shortest such interval [8], [9].

The flow graph created with this block diagram with additional modification regarding the synchronization and controlling the transmitter and receiver was used to perform the field measurements. The synchronization of the transmitter and the receiver was achieved with setting the exact start time on both. With all these settings a 100 Msamples/s sampling rate was achieved by using a single SFP+ connector on the 10 GbE card, i.e. a maximum baseband bandwidth of 45 MHz.

IV. MEASUREMENTS AND RESULTS

Several field measurements were performed in a stationary scenario at the premises of the Faculty of Electrical Engineering and Information Technologies (FEEIT) at the University Ss Cyril and Methodius in Skopje. The stationary target was at a distance of approximately 14 m from the radar.

We did two experiments, where the starting RF carrier frequency was $F_1 = 1.3GHz$ and the difference between the RF frequencies of the subbands was $\Delta F = 45MHz$. M was set to 4. The parameter values used in both measurements are shown in Table I.

TABLE I
PARAMETER VALUES

exp. #	N	Δf (MHz)	τ (μs)	T (μs)	ΔF (MHz)
1	30	1.5	0.33	1.66	45
2	60	0.75	0.67	3.33	45

In our first experiment, within the baseband bandwidth of 45 MHz, we used $N = 30$ frequencies with a frequency step of $\Delta f = 1.5 \text{ MHz}$. In fact, Δf could have been determined from the previously chosen unambiguous range. Note that an unambiguous range of $R_u = 100 \text{ m}$ corresponds to $\Delta f = 1.5 \text{ MHz}$. With $M = 4$ the total radar bandwidth was increased from 45 MHz to 180 MHz, or from $N = 30$ frequencies to $K = 120$ different frequencies.

As mentioned in Section II there are phase jumps in the phase characteristic at the borders of the adjacent subbands. Fig. 2 shows these phase jumps.

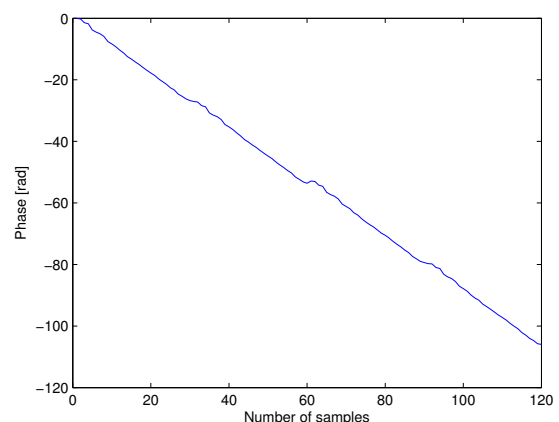


Fig. 2. Phase characteristic for $\Delta f = 1.5 MHz$, $N = 30$, $M = 4$

We took care of these phase jumps by estimating the y -intercept of the linear regression of the phase characteristic in each subband and subtracting this phase estimate, as described in Section II.

In Fig. 3 we show the results for the range profile. The size of the IDFT is $L = 2048$, and, since we have only $K = 120$ measurements, we zero-pad the remaining samples up to 2048. The peak is at the 310-th sample, which corresponds to a target distance of $310/2048 * R_u = 15.14m$ ($R_u = 100m$). By increasing the size of the IDFT, the number of points used for the representation of the range profile increases, but the

resolution does not improve, since we do not have additional measurements.

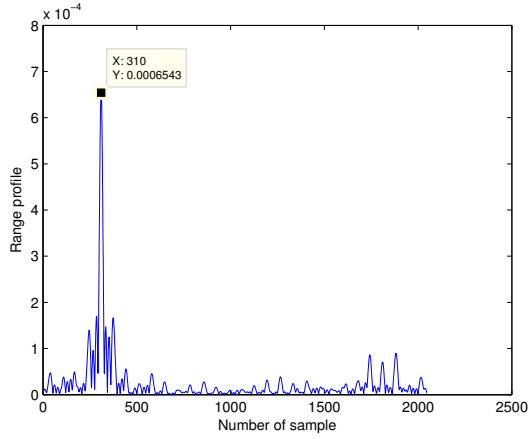


Fig. 3. Range profile for $\Delta f = 1.5 \text{ MHz}$, $N = 30$, $M = 4$

To demonstrate the resolution improvement, in Fig. 4 we show the results for the range profile for the case of a single subband of 1.3 GHz RF frequency.

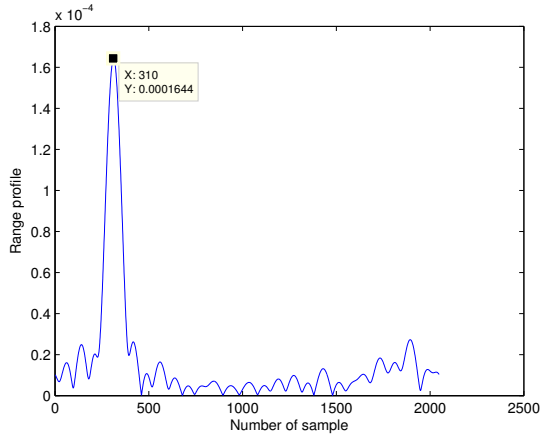


Fig. 4. Range profile for $\Delta f = 1.5 \text{ MHz}$, $N = 30$, $M = 1$

The second experiment used $N = 60$ frequencies in the 45 MHz baseband bandwidth with a step $\Delta f = 0.75 \text{ MHz}$.

In Fig. 5 we show the results for the range profile for the second experiment. The size of the IDFT is $L = 2048$. The peak is at the 158-th sample, which corresponds to a target distance of $158/2048 * R_u = 15.43 \text{ m}$ ($R_u = 200 \text{ m}$).

Compared to the first experiment, the resolution is the same (we have twice as many frequency points, 240 compared to 120, but the unambiguous range is twice as large at 200 m , compared to 100 m). But, the increased unambiguous range is obtained at the price of doubling the number of points, i.e. introducing a larger measurement delay.

V. CONCLUSION

We describe an SF radar approach suitable for a USRP implementation, that combines baseband frequency hopping with

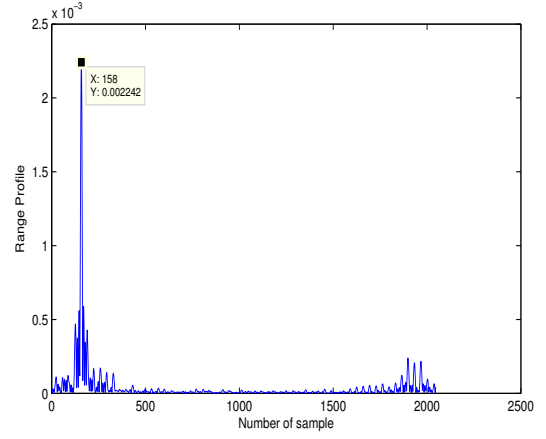


Fig. 5. Range profile for $\Delta f = 0.75 \text{ MHz}$, $N = 60$, $M = 4$

RF frequency hopping. The results show increased resolution, which can be further increased, by increasing the number of subbands throughout the entire USRP frequency range. The only limitation of this approach is the relatively large setting time of the RF frequency, which can be significantly reduced (in the order of 10 times), according to [8], [9]. Also, future work has to address the potential increase of the maximum sampling frequency to reach the maximum theoretically achievable for USRP X310. Another issue that should be addressed is the problem of phase jumps, i.e. its origin, and how to estimate it from the hardware properties. Frequency instability and I/Q imbalance could be possible contributing factors.

ACKNOWLEDGEMENT

The authors express their gratitude to NATO SPS Programme for the support of the presented work provided by the project grant NATO SPS 985208.

REFERENCES

- [1] Mark A. Richards, *Fundamentals of Radar Signal Processing*, Second Edition, Mc Graw Hill, 2014.
- [2] Donald R. Wehner, *High-Resolution Radar*, Second Edition, Artech House, 1995.
- [3] William L. Melvin and James A. Scheer, *Principles of Modern Radar Vol. II: Advanced Techniques*, Scitech Publishing, 2013.
- [4] N. Levanon, Stepped-frequency pulse-train radar signal, *IEEE Proc. Radar, Sonar, Navig.*, Vol.149, No.6, pp. 297-309, Dec. 2002.
- [5] S. Costanzo, F. Spadafora, A. Borgia, H. O. Moreno, A. Costanzo and G. Di Massa, High Resolution Software Defined Radar System for Target Detection, *Journal of Electrical and Computer Engineering*, Vol. 2013, Article ID 573217, 7 pages, Hindawi.
- [6] C. Lopez-Martinez, M. Vidal-Morera, Simulation of FMCW Radar Systems Based on Software Defined Radio, *Proc. of the 6th GNU Radio Conf.*, Boulder, USA, Sep. 2016.
- [7] A. Charisma, A. D. Setiawan, S. A. Rahayu, A. B. Suksmono and A. Munir, Matlab and GNU Radio Based SFCW Radar for Range Detection, *Proc. 5th Int. Conf on Electr. Eng. and Informatics*, Bali, Indonesia, Aug. 2015, pp. 401-404.
- [8] M. Ibrahim and I. Galal, Improved SDR Frequency Tuning Algorithm for Frequency Hopping Systems, *ETRI Journal*, Vol. 38, No. 3, pp. 455-462, June 2016.
- [9] R. Bell, Maximum Supported Hopping Rate Measurements using the Universal Software Radio Peripheral Software Defined Radio, *Proc. of the 6th GNU Radio Conf.*, Boulder, USA, Sep. 2016.